Italian Journal of Engineering Geology and Environment
www.ijege.uniroma1.it

BY-PASS SEDIMENT SYSTEM TO REPLACE LONGSHORE CURRENT IN HARBOUR AREAS

Giuseppe CIANFLONE(*), Gianpietro IMBROGNO(*), Flaubert NGUEBIAPSSI KEMBEU(*), Nadia PENNA(**), Domenico FERRARO(**), Daniele CIRILLO(***), Fabio IETTO(*) & Rocco DOMINICI(*)

(*)University of Calabria - Department of Biology, Ecology and Earth Science - Arcavacata di Rende (CS), Italy
(**)University of Calabria - Department of Civil Engineering - Arcavacata di Rende (CS), Italy
(***)University G. d'Annunzio of Chieti-Pescara - Laboratory of Structural Geology, 3D Digital Cartography and Geomatics - Chieti, Italy
Corresponding author: giuseppe.cianflone@unical.it

EXTENDED ABSTRACT

Il bilancio sedimentario a scala del sistema bacino idrografico-area di costa è molto importante nel sistema di gestione sia delle aree fluviali che di quelle costiere. Nell'ambito del progetto Tech4You (T4Y S2G2PP2), è stata analizzata la problematica dell'insabbiamento dell'imboccatura del porto di Cetraro (Calabria, Italia meridionale). In merito al clima meteomarino, l'unità fisiografica che include il porto di Cetraro è direttamente esposta all'azione di venti provenienti da sud-ovest, ovest e nord-ovest attraverso il Mar Tirreno. Il vento dominante soffia da ovest-sud-ovest con un fetch geografico maggiore di 1650 km e velocità fino a 7 Beaufort (≥ 28 nodi). Queste velocità sono frequenti in inverno e producono le onde più alte fino a 5m. I venti prevalenti sono quelli che provengono da nord-ovest, con un fetch massimo di 650 km e velocità minori di 6 Beaufort (< 22 nodi). Questi venti soffiano prevalentemente durante la primavera e l'estate. Il movimento longshore dei sedimenti, che avviene da nord verso sud, è interrotto dal molo di sopraflutto del porto che causa un consistente processo di accrezione della spiaggia sul lato Nord del porto e insabbiamento alla sua imboccatura (~10,000 m^3/anno di materiale depositato); al contrario, nel tratto di costa sottoflutto, sono stati osservati intensi processi di erosione verosimilmente dovuti alla forte riduzione di apporto sedimentario lungo costa.

Nell'ambito del bilancio sedimentario dell'unità fisiografica, è stata analizzata la produzione di sedimento all'interno del bacino idrografico del Fiume Aron. Quest'ultimo rappresenta la principale sorgente di alimentazione sedimentaria all'interno della stessa unità fisiografica. La potenziale produzione media annua di sedimento del bacino idrografico è stata stimata attraverso il Modello dell'Erosione Potenziale (EPM) di Gavrilovic, utilizzando il plug-in PQGis YES che permette di applicarle l'EPM in modo semi-automatico. L'EPM è un modello semiquantitativo che si basa su dati geologici, geomorfologici, climatici e di uso del suolo. Partendo da questi dati, il modello permette di stimare la potenziale produzione di sedimento del bacino idrografico, il trasporto e la sedimentazione.

L'uso del suolo all'interno del bacino del Fiume Aron è stato mappato mediante l'analisi di immagini satellitari multitemporali e multispettrali utilizzando tecniche machine learning, come l'algoritmo "*Random forest*". I dati ottenuti sono stati successivamente validati da specifiche verifiche di campo. I principali risultati dell'analisi multitemporale hanno mostrato un incremento nel tempo delle aree boschive ai danni delle aree seminative e dedite al pascolo, correlato al progressivo abbandono delle aree rurali. Lungo il settore costiero è stato invece osservato un incremento delle aree urbanizzate. Il coefficiente relativo alla litologia, previsto nel modello EPM, è stato attribuito ai diversi litotipi affioranti nel bacino dopo averne valutato la resistenza attraverso specifici rilievi geomeccanici. Per il bacino del Fiume Aron, la stima del volume medio di sedimenti prodotti annualmente ottenuta con il modello EPM risultata pari a ~30,000 m^3/anno.

La quantificazione dei volumi di sedimento coinvolti nel bilancio sedimentario costiero e la conoscenza delle correnti nel settore sotto costa ha permesso di ideare una soluzione progettuale in grado di mitigare allo stesso tempo l'insabbiamento dell'imboccatura del porto e i processi di erosione nell'area sottoflutto. Nel dettaglio, è stato progettato un sistema di *bypass* consistente in una pompa sommersa, da installare nella porzione finale del molo nel settore sopraflutto, avente lo scopo di dragare autonomamente il materiale sedimentario accumulato e riversarlo nel tratto di costa a sud del porto. Il sistema di *bypass* permette quindi di movimentare autonomamente il sedimento dalla trappola generata dalla struttura portuale nel settore costiero sottoflutto. In pratica, il sistema permette di riattivare artificialmente la naturale corrente di longshore interrotta dalla costruzione del porto. Contemporaneamente è stato sviluppato anche un sistema di monitoraggio che permette di valutare l'impatto del funzionamento del *bypass* sulle diverse matrici ambientali.

IJEGE, Special Issue 1 (2024): 57-67, DOI: 10.4408/IJEGE.2024-01.S-07
E-ISSN 2035-5688 | ISSN 1825-6635 /

ABSTRACT

This paper is part of the results achieved in Tech4You project T4Y S2G2PP2 funded by PNRR (Piano Nazionale di Ricerca e Resilienza). The Tech4You project focused on the silting process affecting the Cetraro harbour mouth (Calabria, southern Italy). The study area is located along the northern Calabrian Tyrrhenian coast and is part of a physiographic unit with a west-southwest fetch greater than 1650 km. The wave climate is characterised by a significant wave height of 0.65m (average period of 5.15s) and 1.01 m (average period of 5.7s) offshore and inshore, respectively. The longshore flow of sediments (about 80,000 m^3/yr), moving from north to south, is interrupted by the harbour pier producing silting (~10,000 m^3/yr sediment deposited at the harbour mouth), and heavy coastal erosion in the down-drift sector. The sediment production in the Aron River catchment (representing the main sediment feed in the physiographic unit) by Gravrilovic model was also studied, with detailed analysis of soil use through multispectral analysis, and estimate an average volume of ~30,000 m^3/yr. A bypass system was designed, consisting of a submerged pump installed at the end of the pier on the up-drift side of the harbour, to replace the original longshore current, contrasting simultaneously both mouth silting and erosion processes in the down-drift coastline.

KEYWORDS: sediment management, dredging, sustainable harbours.

INTRODUCTION

Coastal erosion currently affects much of the worldwide Nation, in particular areas characterised by the presence of widespread anthropic structures (*e.g.* ANFUSO & DEL POZO, 2005; STANCHEVA *et alii*, 2011; IETTO *et alii*, 2018).

Anthropogenic pressure is a serious problem affecting many coastal areas (*e.g.*, ALVAREZ-CUESTA *et alii*, 2021; IETTO *et alii*, 2014).

The coastal anthropization area has increasingly accelerated in the second half of the twentieth century (e.g., IETTO *et alii*, 2014; CANTASANO *et alii*, 2017). In fact, after the end of the Second World War, a considerable migration from inland to coastal territories was observed in most coastal areas in the Mediterranean region (ROMANO *et alii*, 2017). It is significative for example, the number of coastal cities, that is quintupled in the last 70 years, and the percentage of the population living close to the coastal areas which is about 20% of the world population (*e.g.* STRONKHORST *et alii*, 2018)

The anthropogenic pressure produced a disequilibrium in both coastal and river environments, that represents the trigger of the shoreline erosion processes (*e.g.* BOMBINO *et alii*, 2022; FOTI *et alii*, 2022). On coastal areas it mainly includes the construction of new settlements (often substituting beaches and dune systems), expanding existing coastal towns, and the construction of port and coastal structures (*e.g.*, CANTASANO *et alii*, 2023). Furthermore, in the fluvial environments, anthropogenic structures such as dams and weirs represent traps for the bedload transport, producing consequently a deficit in the sedimentary balance of the littoral areas.

FOTI *et alii* (2022) analyzed urban expansion along the Calabrian coasts during the last 70 years, showing an increase of urban centers from 32 to 83, with an increase of urbanized area from 15 km^2 to 250 km^2. The same authors, in according to previous researchers (D'ALESSANDRO *et alii*, 1998, 2002; IETTO, 2001; GUIDUCCI & PAOLELLA, 2004), highlighted that the increase of urbanisation triggered widespread coastal erosion phenomena. In detail, the main erosive effects are recorded along the northern Tyrrhenian coast (Figure 1a,b), which represents the pilot area of this study. In particular, this research studied the coastal area surrounding Cetraro village in Cosenza province (southern Italy, Figure 1c), where the morphological evolution was investigated through the scientific literature. In detail, IETTO (2001) reconstructed and interpreted the shoreline evolution of the northern Tyrrhenian Calabrian coast between 1953 and 1999, showing a shoreline retreat rate of 0,9÷1 m/yr in the period 1953-1983, with a deceleration in the subsequent period 1983-1999. Referring to the Cetraro Marina area, the same Author showed a shoreline retreat of 120 m in the period 1953-1983, followed by an advance of 12 m in the period 1983-1999, he highlights a shoreline advance of 40 m, during the period 1954-1983, in correspondence with the Cetraro harbour up-drift side. Furthermore, IETTO *et alii* (2018) argued on a new coastal erosion risk assessment indicator applied to the northern Tyrrhenian sector. They showed that 35% of the coastal sector could be classified as very high risk, 30% as high risk, 28% as medium risk and only 7% as low risk.

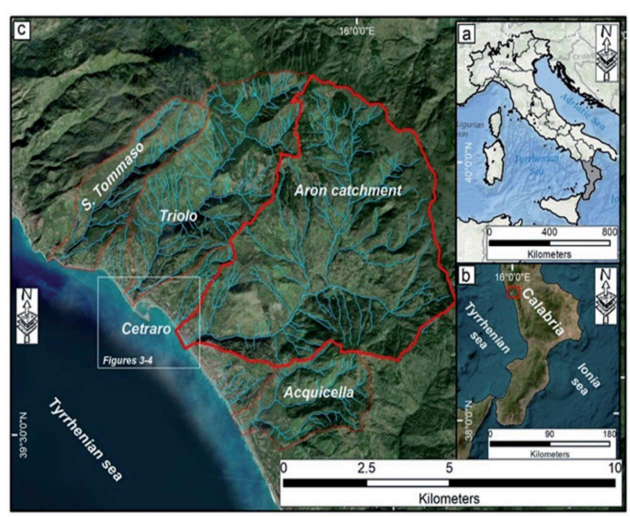

Fig. 1 - Location of the study area. a) location of Calabria (greyish colour) region in southern Italy; b) Location of the studied area in the northwestern part of the Catena Costiera Calabra (red rectangle); c) Bold Red polygon represents the Aron River catchment and in light blue lines its tributaries, also represented the adjacent S. Tommaso Triolo and Acquicella catchments

In this context, the present research focuses on the silting process affecting the Cetraro harbour mouth. In detail, the aim of the study, part of the Tech4You project (T4Y S2G2PP2), consists of the design of a bypass system that allows the movement of sediments from the artificial obstruction created by the harbour structure to the down-drift coastline. Usually, the consolidated method to remove the deposited material in the harbour mouth consists of the dredging process, allowing the correct navigation. However, this process has some drawbacks: (*i*) relatively high and low predictable costs; (*ii*) significant impact on marine flora and fauna; (*iii*) mobilization of pollutants already present on the seabed. This research proposed a technological solution consisting of a permanently submerged pump close to the harbour mouth, allowing more efficient management of sediments which are moved to the down-drift coastline.

GEOLOGICAL SETTING

The study area is located along the northern Tyrrhenian coast of the Calabria region, between the mouth of Noce and Savuto rivers, which flow northward and southward, respectively.

The studied littoral sector extends mainly at the foot of the Pollino Massif (north-northward) and Catena Costiera (southward) (Figure 2).

The surrounding area's geological setting is mainly represented by different tectonostratigraphic units belonging to different paleographic domains (Figure 2). Seven tectono-stratigraphic units outcropping in the northern Calabria region, from the bottom to the top: *i*) Lungro-Verbicaro unit consituited by Meso-Cenozoic metamorphic carbonatic and pelitic sedimentary successions (Iannace *et alii* 2007); *ii*) Pollino-Ciagola units that overlay the Lungro-Verbicaro unit, and it is mainly rappresented by a typically Apenninic carbonate platform succession of the late Triassic to Cretaceous dolostone and limestone covered in discordance by Paleogenic and Neogenic sedimentary succession locally intruded by Miocenic pillow lavas (Amodio-Morelli *et alii*, 1976; Iannace *et alii*, 2007); *iii*) Ligurian unit, that consist of ophiolitic sequences and deep-sea deposits derived from the western Thethys oceanic basin (Amodio-Morelli *et alii*, 1976; Filice *et alii*, 2015); *iv*) Castagna unit that consists of a ductiles shear zone of rocks between the contact of Liguride unit and the base of the upper overlayed Sila unit (Amodio-Morelli *et alii*, 1976; Filice *et alii*, 2015); *v*) Sila unit consist in the continental units, representative of both lower and upper levels of the continental crust and small volumes of subcontinental upper mantle rocks of the Variscan orogeny (Liberi *et alii*, 2011; Piluso & Morten, 2004; Piluso *et alii*, 2000); *vi*) Miocenic succession consist in a clays, arenites and conglomerates of Serravallian to evaporites deposits of Messinian ages (Mattei *et alii*, 2002); *vii*) Plio-Quaternary deposits mainly represented by different cronhostratigraphic sequences composed by a clays, sands and conglomerates of fan deltas deposits, marine and fluvial terraces deposits, until eluvio-colluvial and by stream river and beach deposit of Holocene (Brozzetti *et alii*, 2017).

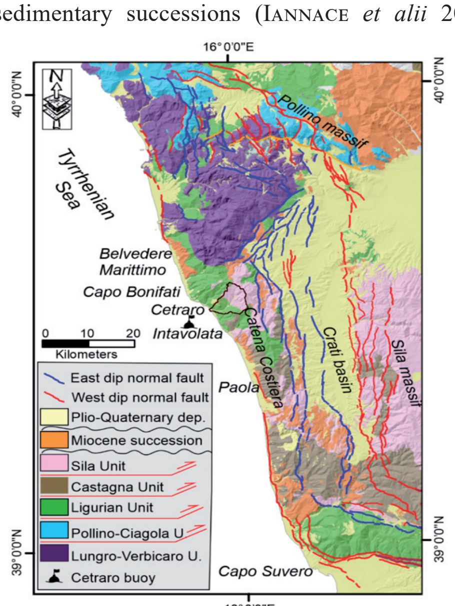

Fig. 2 - Geological map of the northern Calabria modified after Geological Map 25,000 CasMez Calabria (tectono-stratigraphy) and from Lavecchia et alii, 2024 (Quaternary Faults)

The actual physiography of the northern Calabria is guided by the activities of the Quaternary and active faults that drive the uplift of the structural high as Pollino massif, like the horst of the Catena Costiera and the Sila Massif, and the subsidence of the Crati and Paola basins (Brozzetti *et alii,* 2017; Cirillo *et alii,* 2022). The combining of the uplift, the weathering, the erosion and the landslides and rockfall play a fundamental role in terms of sediment production for the subsequent transportation from the riverbed to the beach in the Calabria shoreline areas (Cianflone *et alii*, 2021; Tangari *et alii*, 2021; Ietto *et alii*, 2022; Cirillo *et alii*, 2024).

The study area is included in the Paola physiographic unit (Lisi *et alii*, 2010). This is delimited by Capo Bonifati and Capo Suvero promontories northward and southward respectively. This physiographic unit has a length of about 150 km and a depth of closure between -7.6 and -9.9 m a.s.l. The study area can be included in the northern subsector of the Paola physiographic unit, delimited to the north and south by Capo Bonifati and Intavolata promontories respectively. This sector is characterised by longshore dowdrift from north to south and manly coarse sediment supply related to S.Tommaso, Triolo, Aron and Acquicella streams (Fig. 1c) (CNR, 1997).

METHODS

The design of the bypass technological solution needed a multidisciplinary approach involving different technical skills. In fact, the different topics analysed in this research included: (*i*) wave and current regime; (*ii*) morphological and sedimentological analysis of the beach sediments in backshore and offshore areas; (*iii*) sediment balance (including longshore sediment transport and fluvial sediment discharge); (*iv*) environmental impact of the sediment movement referring to the Italian legislation; (*v*) submerged pump technology.

The analysis of wave climate was based on wave dataset (from 1999 to 2008) acquired by the Cetraro Buoy (lat. 39.453, long. 15.918), belonging to the Italian National Sea Wave Measurement Network (RON - Bencivenga *et alii*, 2012). The dataset collected by the buoy includes: significant wave height, period, and direction at intervals of 30 min.

The analysis of past storm surges identified significant wave heights. The meteorological analysis focused on surface wind, using data from the Belvedere Marittimo and Paola stations.

The analysis of the morphological evolution of submerged areas was based on multi-temporal maps (1954), aerial photos (1985, 1998, 2008) and satellite image (2023). For the submerged area, a multibeam survey has been realized by means of the survey boat of the Marine Laboratory DiBEST-SILA (Unical) equipped with a Multibeam Echosounder Norbit WBMS Basic (400kHz).

The study of littoral transport was based on the calculation realized in the Coastal Master plan of the Calabria Region. This calculation was performed using the model UNIBEST CL+ developed by Delt University. The model, which is not discussed in depth, takes into account different elements: (*i*) altitude profile of the beach; (*ii*) wave climate and marine currents; (*iii*) parameters of wave transformation and breaking; (*iv*) grain size sediment parameters (D50 and D90). In the same masterplan, the sediment balance was calculated considering: (*i*) the fluvial sediment discharge; (*ii*) the littoral transport; (*iii*) beach nourishment and sand extraction; (*iv*) offshore sand loss. Starting from this calculation of sediment balance, only the volume of fluvial sediment discharge was modified (see later).

The estimation of the sediment balance in the littoral cell took into account the volume of sediments deposited in the nearshore area (estimated by multibeam survey) and fluvial sediment discharge. For the estimation of the sediment yield and erosion intensity at the basin scale, the erosion potential method (EPM) was used. The EPM (Gavrilovic, 1988) estimates the average annual specific production of sediments (W) in m^3/yr through the following equation:

$$W = Th\pi S\sqrt{(Z^3)}$$

Where T is the temperature coefficient calculated from the mean annual air temperature (°C); h is the mean annual precipitation (mm/years); S is the watershed area (km^2); Z is the erosion coefficient:

$$Z = XY(\gamma+\sqrt{Im})$$

Where X is the land use coefficient; Y is the coefficient of the rock and soil resistance (a function of geology and soil type); γ is the coefficient of type and extent of erosion; *Im* is the average slope steepness of the watershed (%).

The EPM analysis provides an estimated sediment production for the entire catchment area (or at the closure points of individual river basins), but it does not indicate the sectors with different sediment production. To address this, the YES plug-in (Dominici *et alii*, 2020) was employed based on GIS techniques and the subdivision of the catchment into a grid matrix. The "squared cell" method calculates sediment production by applying an algorithm to each individual cell.

Different rasters were therefore created containing different information representing the main parameters entering the model and the estimation of sediment yield performed.

In this study, the coefficients of soil resistance to erosion (Y) were assigned using the methodology proposed by Zemljic (1971). The values were obtained from the Calabria geological map at the scale 1: 25,000.

The coefficient of type and extent of erosion (γ) was obtained using the methodology proposed by Zemljic (1971) on the data from PAI (the Hydrogeological Plan of southern Italy, https://gn.mase.gov.it/portale/wfs).

The average slope of the watershed (Im) was calculated using a DEM of the basin area, with cell size of 20 × 20 m (http://wms.pcn.minambiente.it/wcs/dtm_20m), reclassifying the values into five categories between 0 and 1 (Gavrilovic, 1988).

T and h were obtained from the ISPRA database. (https://www.isprambiente.gov.it/pre_meteo/idro/BIGBANG_ISPRA.html).

Subsequently, the average annual specific production of sediment (W) was calibrated with an innovative approach based on the calibration of the land use parameter through multispectral satellite data processing techniques.

To obtain an accurate estimate of sediment production, the land use coefficient (X) was analyzed using highly updated multispectral data and dividing the values into seven categories (Zemljic, 1971). The image processing was carried out using the particular calculation algorithm Random Forest (RF) (Ho, 1995; Breiman, 2001). This classifier is an aggregation of a set of decision trees and is based on two fundamental principles: bagging and random subspace. During the construction of the RF classifier, it is therefore necessary to set various parameters such as the number of decision trees and the number of elements on which to train the algorithm.

The procedure involves the use of a supervised classification in which different training areas or Regions Of Interest (ROIs) are identified with which the algorithm is oriented. More than 100 different ROIs were identified, divided by single spectral signature and processed using the SCP plug-in (Congedo, 2021) present in the QGIS platform.

The scheme with which the entire procedure was developed provides for the extraction of individual spectral signatures, for each land use category, and their subsequent use in the final classification. The coefficients calculated as previously described were used to carry out the calculation through the EPM model.

The potential environmental impact of the proposed technical solution was investigated by means of: (*i*) sediments sampling in both emerged and submerged sites; (*ii*) 2 multiparametric seawater column logs including measurements of: temperature, pH, turbidity, dissolved oxygen concentration, salinity, density, transparency, fluorescence, and suspended solids. The logs were acquired during May and October 2023 using the multiparametric probe Ocean Seven 316Plus (Idronaut). The turbidity meaurements were collected following the protocols: a) method 180.1 of United States Environmental Protection Agency (EPA) (1993) and (b) American Public Health Association - American Water Works Association - Water Environment Federation - Standard Methods for the Examination of Water and Wastewater (1999).

The four sediment samples were subjected to sedimentological identification and characterization and ecotoxicological (referring to Apat-Icram, 2007) analysis.

RESULTS AND DISCUSSION

To analyse the morphological evolution of the coastal area, multi-temporal coastlines from geographic maps, aerial photos and satellite images were compared (Figure 3). The first comparison is between 1958 (from the Casmez geographic map) and 1985 (from FS-Casmez aerial photo), showing in the up-drift sector with respect to the harbour structure, a coastline increasing with a local maximum of 35 m. Instead, the coastline retreated up to 100 m in the down-drift sector. Between 1985 and 1998 (aerial photo ITA2000 fly), the up-drift sector was characterised by tracts with metric coastline progress and retreat, except the coast stretch close to the harbour breakwater where the coastline progressed up to 50 m. During the same period, also the down-drift sector was characterised by a coastline progress up to 40 m. Between 1998 and 2008 (from aerial photo of Calabria Region), in the up-drift sector 2, coast portions characterised by retreat (up to 25 m) in the northward area and progress (up to 25 m) in the southward were observed. The down-drift sector is instead characterised by coastline retreat up to 17 m. During the period 2008-2023 (from Sentinel-2 satellite image) a general coastline retreat (up to 30 m) in the northern and up-drift sector was observed. Local coastline retreat was also observed in the down-drift sector. Close to the harbour mouth was estimated a deposition of about 10,000 m^3/yr of sediments.

In the studied area, the evolution of the coastline was hardly influenced by anthropogenic activities. In fact, in the period 1959-1985, the coastline progress and retreat, respectively, in the up-drift and down-drift sectors (with respect to the harbour) can be related to the Cetraro harbour construction that happened during the 1960s. From 1985 to 1998, the relevant coastline progress close to the northern breakwater can be related to the west pier prolongation (realised to contrast the mouth siltation). Instead, the local coastline progress in the downdrift sector can be ascribed to the realisation of coastal defence measures (beach nourishment and longitudinal emerged breakwaters). Between 1998 and 2008, the up-drift sector continued the coastline progress, while in the down-drift one the coastline retreat persisted despite the realization of new longitudinal emerged breakwaters. Finally, the general coastline retreat can be ascribed to a deficit in the sediment balance due to less solid fluvial discharge related to the variation of land use in the river catchment (see later) and the realisation of hydraulic works along the drainage network.

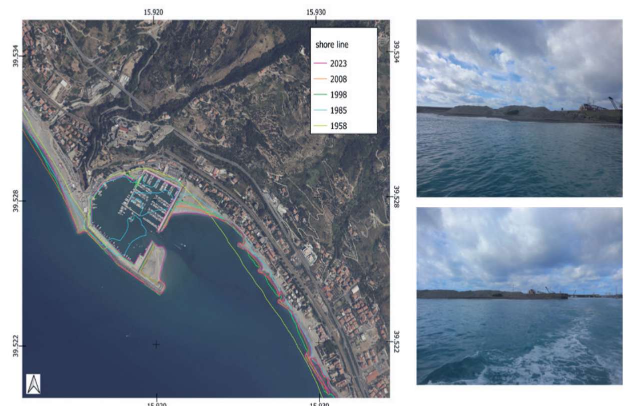

Fig. 3 - Multi-temporal coastlines and photo of deposits at the harbour mouth

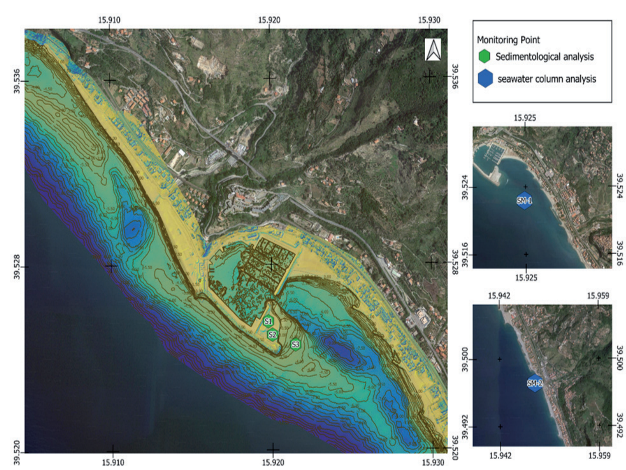

Fig. 4 - Multibeam survey and location of sediments samples (S1, S2, S3) and seawater column multiparametric logs (SM1, SM2)

The multibeam survey allowed to obtain a 1×1 m grid (Figure 4). In the northern sector, up-drift with respect to the harbour, a northwest-southeast bar with a height up to 1.5 m (from –4 to –2.5 m a.s.l.) can be observed. This bar is separated from the coastline by a through deep up to -5.5 m a.s.l.; southward, the bar is limited by another through deep up to -8 m a.s.l. Close to the northern harbour breakwater, a more extended surf zone occurs, about 160 m long between -4.5 and -5.5 m a.s.l. Interesting features can be observed southward from the pier, where a northwest-southeast bar, high up to 5 m (from -9 to -4 m a.s.l.) represents the prolongation of the same pier. The bar is separated from the coastline by a deep up to -9 m a.s.l. In the southern sector, we observed a more extended surf zone, about 150 m long between -4.5 and -5.5 m a.s.l.

The marine weather in the physiographic unit, including the Cetraro harbour, is directly exposed to wind action from southwest, West and North-West across the Tyrrhenian Sea. The dominant wind blows from the west-southwest direction with a geographical fetch greater than 1650 km and speeds up to 7 Beaufort (≥ 28 knots). They are frequent in winter, producing the highest sea waves up to more than 5 m. The winds from the northwest are prevailing winds with a maximum fetch of 650 km and speeds less than 6 Beaufort (< 22 knots). They blow mainly in the spring and summer seasons. The longshore flow of sediments, moving from north to south, is interrupted by the harbour dock.

The data acquired by the Cetraro Buoy show a significant wave height of 0.65 m with an average period of 5.15 s. Inshore, the wave climate calculated is characterised by an average energy flux of 6.1 kN/s and a significant wave height of 1.01 m with an average period of 5.7 s.

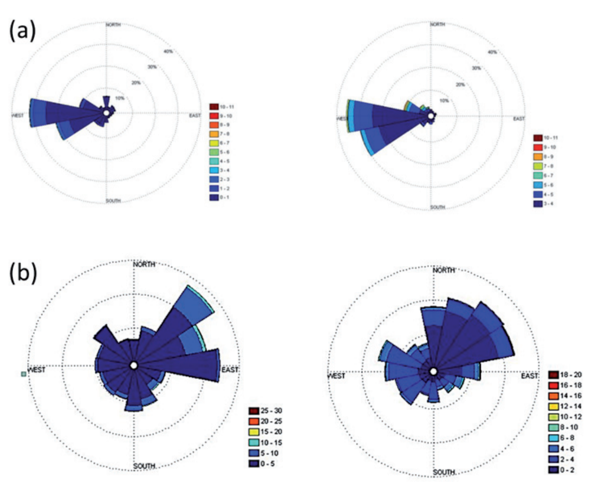

Fig. 5 - Frequency distribution of wave height and mean direction. (b) Wind behavior at the Paola (left rose diagram) and Belvedere (right rose diagram) stations

The application of EPM model to estimate the potential sediments yield of the Aron River catchment was based on bibliographic data (geological and landslide maps, thermal-pluviometic data, DEM). However, some coefficients included in the EPM calculation were calibrated by in situ measurements. In detail, the *Y* coefficient of the EPM, depending by the rock and soil resistance, was assigned to the different lithotypes cropping out in the catchment area based on 9 geomechanical surveys. During the geomechanical surveys, realized on the rock masses of the different lithotypes, the dips, dip directions and strikes, spacing, length, aperture, and joint roughness coefficient (JRC) of discontinuities were measured. Furthermore, the Schmidt hammer rebound value was measured, and the Geological Strength Index (GSI - Hoek & Brown, 1997) was estimated. Qualitative observations about the weathering of different lithotypes were realized.

At this step, the calculation with the EPM was carried out by keeping all the coefficients fixed (*Y*, *y*, *Im*, etc.) and making only the *X* coefficient (depending on land use) vary. The first calculation was performed using the Corine Land Cover 2012 land use map for the assignment of *X* coefficient. A second calculation was realized with the values assigned to the new land use classes coming from the processing of multispectral data (Land-Use 2023). In both cases, the values of the coefficients were assigned as proposed by Zemljic, 1971. The different types of land use were redefined by means of multispectral analysis techniques. In detail, we used a classifier such as Random Forest, which performs well for multi-source classification of geographic and remote sensing data (Gislason *et alii*, 2006).

In the first calculation, the value of *W* (average annual specific production of sediments) is equal to 29900 m^3/year, while in the second one, it is equal to approximately 23600 m^3/year. The difference between the values can be related to the degree of detail in defining the polygons with which the two land use classifications were created. In the case of the Corine Land Cover 2012, approximately 90 polygons differentiated into 10 main classes were identified in the Aron River. In the land use processed from multispectral data, more than 400 polygons divided into 18 classes were identified. It follows that the error in assigning coefficients to individual classes decreases greatly because each coefficient is applied to extremely homogeneous areas in terms of land use. Furthermore, comparing the two land use maps, it is possible to evaluate a decrease in the cultivated areas between 2012 and 2023, and consequently, an increase in the wooded areas.

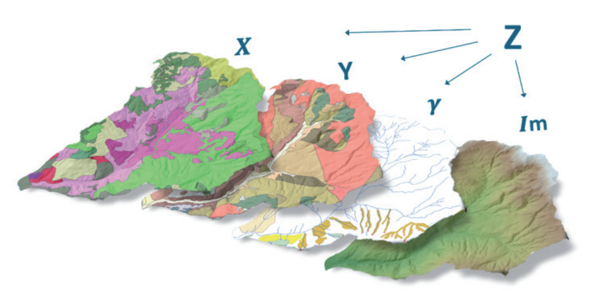

Fig. 6 - EPM coefficients relate to soil-use (X), lithology (Y) and geo-morphology (γ and Im)

The results of this preliminary study on the impact of land use in estimating sediment production highlight some extremely interesting aspects on which further research can be carried out:

Station	Data	Depth	Temperature	Conductivity	Salinity	Oxygen (OPTsat)	Oxygen (OPTppm)	pH	Eh	Turbidity
S1	May-2023	0.75	21.7468	56.1068	38.1431	97.9	6.61	8.0805	407.2	66.156
		1	21.7471	56.1061	38.1423	97.9	6.62	8.0785	408.9	65.859
		1.25	21.75	56.1123	38.1436	97.9	6.62	8.0775	409.5	65.772
		1.5	21.7333	56.0867	38.1408	97.9	6.62	8.0765	410.6	65.598
		1.75	21.7315	56.0872	38.1409	97.9	6.62	8.0755	411.7	65.566
		2	21.7322	56.0911	38.1433	98	6.62	8.0735	412.8	63.579
		2.25	21.7396	56.099	38.1445	98	6.62	8.0725	413.8	61.534
		2.5	21.7403	56.1028	38.1451	98	6.62	8.0715	414.5	60.525
		2.75	21.7409	56.1015	38.1435	98	6.62	8.0705	414.9	60.514
		3	21.7417	56.1001	38.1416	98	6.62	8.0635	415.4	58.548
		3.25	21.7426	56.1022	38.1423	98	6.62	8.0665	416.3	57.515
		3.5	21.7434	56.1054	38.1441	98	6.63	8.0685	417.2	55.626
		3.75	21.7424	56.1009	38.1413	98	6.63	8.0575	417.7	55.694
		4	21.7407	56.1	38.142	98	6.62	8.0655	418.4	54.636
		4.25	21.74	56.1018	38.144	98.1	6.63	8.0665	419.3	52.578
		4.5	21.7398	56.0993	38.1421	98.1	6.63	8.0645	419.9	51.29
		4.75	21.7396	56.096	38.1397	98	6.63	8.0635	420.3	49.595
		5	21.7377	56.0964	38.1415	98	6.63	8.0615	420.7	48.615
		5.25	21.7363	56.0934	38.1403	98.1	6.63	8.0605	421.1	47.346
		5.5	21.734	56.0897	38.1394	98.1	6.63	8.0605	421.5	47.184
		5.75	21.7322	56.0829	38.1365	98.2	6.64	8.0575	422.1	46.941
		6	21.7335	56.0796	38.1319	98.3	6.64	8.0375	425	46.182
		6.15	21.7358	56.0634	38.1174	98.2	6.64	8.0585	434	45.906
S2	May-2023	0.5	22.112	55.83911	37.92965	102.5	7.57	7.704	208.6	25.924
		0.75	22.1155	55.85513	37.93806	100.2	6.96	7.769	202.4	21.387
		1	22.1184	55.85563	37.93756	99.2	6.71	7.826	197.4	19.95
		1.25	22.1227	55.86885	37.94317	99	6.7	7.831	196.3	19.756
		1.5	22.1214	55.87376	37.94788	99	6.7	7.847	196.1	19.739
		1.75	22.1219	55.88597	37.95669	99.2	6.71	7.848	195.4	19.832
		2	22.1189	55.88697	37.95999	99.3	6.72	7.854	194.9	19.744
		2.25	22.1202	55.89248	37.9639	99.4	6.72	7.863	194.6	19.745
		2.5	22.1163	55.89638	37.9684	99.4	6.72	7.868	194.1	19.782
		2.75	22.1223	55.90109	37.9676	99.5	6.73	7.881	193.1	19.554
		3	22.131	55.9123	37.9688	99.4	6.72	7.912	191.9	19.63
		3.25	22.1287	55.9109	37.9696	99.4	6.72	7.914	191.8	19.737
		3.5	22.1288	55.91891	37.97551	99.4	6.72	7.906	191.7	19.567
		3.75	22.1306	55.92612	37.97942	99.4	6.72	7.911	191.6	19.184
		4	22.1294	55.92512	37.97952	99.5	6.73	7.928	191	18.711
		4.25	22.1321	55.9094	37.97371	99.5	6.73	7.934	190.6	18.183
		4.5	22.1312	55.93193	37.98562	99.6	6.73	7.943	190.3	17.943
		4.75	22.1201	55.92842	37.98973	99.5	6.73	7.958	190	17.831
		5	22.1192	55.94094	38.00014	99.5	6.73	7.954	190	17.751
		5.25	22.1162	55.94605	38.00645	99.5	6.73	7.957	189.9	17.744
		5.5	22.1178	55.95275	38.01015	99.5	6.73	7.959	189.9	17.751
		5.75	22.1152	55.95736	38.01416	99.6	6.73	7.962	189.9	17.737
		6	22.1201	55.96998	38.02117	99.6	6.73	7.964	189.9	17.148
		6.25	22.1252	55.98209	38.02868	99.5	6.73	7.963	189.8	16.767
		6.5	22.1261	55.9901	38.03138	99.5	6.73	7.964	189.8	16.142
		6.75	22.1316	56.00862	38.04079	99.6	6.73	7.969	189.7	15.76
		7	22.1314	56.01884	38.0487	99.6	6.73	7.971	189.8	15.045
		7.25	22.1304	56.02294	38.0509	99.6	6.73	7.973	189.6	14.742
		7.5	22.1312	56.02875	38.05631	99.6	6.73	7.975	189.6	13.727
		7.75	22.1318	56.03946	38.06392	99.6	6.73	7.976	189.6	12.943
		8	22.1382	56.05538	38.07303	99.6	6.73	7.98	189.5	12.129
		8.25	22.1353	56.07531	38.08825	99.6	6.73	7.98	189.5	11.645
		8.5	22.1358	56.09033	38.09916	99.6	6.73	7.979	189.5	11.148
		8.75	22.1339	56.09914	38.10747	99.7	6.73	7.982	189.5	11.04
		9	22.1314	56.11285	38.11839	99.7	6.73	7.981	189.5	10.969
		9.25	22.1349	56.12657	38.1275	99.6	6.73	7.983	189.4	10.877
		9.5	22.1392	56.13939	38.13531	99.6	6.73	7.986	189.4	10.754
		9.75	22.141	56.15641	38.14502	99.7	6.73	7.986	189.4	10.668
		10	22.1412	56.16792	38.15363	99.7	6.73	7.986	189.4	9.446
		10.25	22.1441	56.18084	38.16094	99.7	6.73	7.987	189.4	9.214
		10.55	22.1465	56.21128	38.18207	99.5	6.72	8.009	189.5	9.094

Tab. 1 - Results of the multiparametric logs in the point SM1 and SM2 during May 2023

Station	Data	Depth	Temperature	Conductivity	Salinity	Oxygen (OPTsat)	Oxygen (OPTppm)	pH	Eh	Turbidity
S1	October-2023	0.75	23.9319	56.1068	38.1696	97.9	6.61	8.105	409.9	1.351
		0.75	23.9319	56.1068	38.1696	97.9	6.61	8.105	409.9	1.351
		1	23.9322	56.1061	38.1688	97.9	6.62	8.103	411.6	1.054
		1.25	23.9361	56.1123	38.1701	97.9	6.62	8.102	412.2	0.967
		1.5	23.9164	56.0867	38.1673	97.9	6.62	8.101	413.3	0.793
		1.75	23.9166	56.0872	38.1674	97.9	6.62	8.1	414.4	0.761
		2	23.9173	56.0911	38.1698	98	6.62	8.098	415.5	0.774
		2.25	23.9227	56.099	38.171	98	6.62	8.097	416.5	0.729
		2.5	23.9254	56.1028	38.1716	98	6.62	8.096	417.2	0.72
		2.75	23.926	56.1015	38.17	98	6.62	8.095	417.6	0.709
		3	23.9268	56.1001	38.1681	98	6.62	8.088	418.1	0.743
		3.25	23.9277	56.1022	38.1688	98	6.62	8.091	419	0.71
		3.5	23.9285	56.1054	38.1706	98	6.63	8.093	419.9	0.821
		3.75	23.9275	56.1009	38.1678	98	6.63	8.082	420.4	0.889
		4	23.9258	56.1	38.1685	98	6.62	8.09	421.1	0.831
		4.25	23.9251	56.1018	38.1705	98.1	6.63	8.091	422	0.773
		4.5	23.9249	56.0993	38.1686	98.1	6.63	8.089	422.6	1.485
		4.75	23.9247	56.096	38.1662	98	6.63	8.088	423	0.79
		5	23.9228	56.0964	38.168	98	6.63	8.086	423.4	0.81
		5.25	23.9214	56.0934	38.1668	98.1	6.63	8.085	423.8	1.341
		5.5	23.9191	56.0897	38.1659	98.1	6.63	8.085	424.2	2.379
		5.75	23.9163	56.0829	38.163	98.2	6.64	8.082	424.8	1.136
		6	23.9186	56.0796	38.1584	98.3	6.64	8.062	427.7	1.377
		6.15	23.9209	56.0634	38.1439	98.2	6.64	8.083	436.7	2.101
S2	October-2023	0.5	23.9803	56.1074	38.1286	98.7	6.66	8.075	190.1	0.531
		0.75	23.9818	56.1148	38.133	98.7	6.66	8.07	190.1	0.357
		1	23.9861	56.116	38.1301	98.7	6.66	8.065	190.2	0.298
		1.25	23.9919	56.1333	38.1382	98.7	6.66	8.068	190.1	0.278
		1.5	23.9961	56.1425	38.1417	98.8	6.67	8.065	190	0.357
		1.75	24.0017	56.1516	38.1438	98.7	6.67	8.061	190	0.272
		2	24.0016	56.1513	38.1435	98.7	6.66	8.061	190	0.299
		2.25	24.0013	56.1513	38.1437	98.8	6.67	8.059	189.9	0.312
		2.5	23.9936	56.1421	38.1431	98.7	6.67	8.057	189.9	0.294
		2.75	23.9876	56.1322	38.1406	98.8	6.67	8.055	189.9	0.25
		3	23.9875	56.1356	38.1432	98.8	6.67	8.056	189.8	0.273
		3.25	23.9894	56.1381	38.1434	98.8	6.67	8.056	189.8	0.349
		3.5	23.9843	56.1353	38.1454	98.8	6.67	8.055	189.8	0.288
		3.75	23.9839	56.1282	38.1404	98.8	6.67	8.051	189.8	0.333
		4	23.9911	56.1434	38.1457	98.9	6.68	8.051	189.8	0.274
		4.25	23.9934	56.146	38.1456	99	6.68	8.051	189.8	0.258
		4.5	23.9958	56.1484	38.1453	99	6.69	8.047	189.8	0.268
		4.75	23.9948	56.1476	38.1455	99	6.68	8.048	189.8	0.286
		5	23.9941	56.146	38.1448	98.9	6.68	8.049	189.7	0.534
		5.25	23.9914	56.144	38.1455	99	6.68	8.045	189.7	0.28
		5.5	23.9871	56.1387	38.145	99	6.69	8.042	189.8	0.242
		5.75	23.9872	56.1384	38.1446	99.1	6.69	8.047	189.7	0.249
		6	23.987	56.1387	38.1449	99.1	6.69	8.05	189.7	0.443
		6.25	23.9872	56.1389	38.1448	99.1	6.69	8.044	189.8	0.365
		6.5	23.9866	56.1395	38.1457	99.1	6.69	8.044	189.8	0.238
		6.75	23.9871	56.1399	38.1455	99.1	6.69	8.041	189.7	0.261
		7	23.9853	56.1387	38.146	99.1	6.69	8.039	189.7	0.264
		7.25	23.9823	56.1347	38.1455	99.2	6.7	8.043	189.8	0.276
		7.5	23.981	56.1329	38.1452	99.2	6.7	8.042	189.7	0.241
		7.75	23.9804	56.1295	38.1429	99.2	6.7	8.04	189.7	0.245
		8	23.9802	56.1278	38.1417	99.2	6.7	8.036	189.7	0.252
		8.25	23.9802	56.1334	38.1459	99.3	6.7	8.036	189.7	0.24
		8.5	23.9819	56.1342	38.1449	99.3	6.71	8.037	189.7	0.259
		8.75	23.9855	56.14	38.1462	99.4	6.71	8.034	189.8	0.272
		9	23.9885	56.141	38.1444	99.4	6.71	8.037	189.7	0.268
		9.25	23.9967	56.1506	38.1446	99.5	6.72	8.037	189.9	0.247
		9.5	24.002	56.1568	38.1447	99.5	6.72	8.03	189.7	0.279
		9.75	24.0024	56.1568	38.1443	99.5	6.72	8.016	189.8	0.287
		10	24.0018	56.1561	38.1442	99.4	6.71	8.026	189.8	0.331
		10.25	24.0011	56.1548	38.1437	99.4	6.71	8.033	189.8	0.282
		10.55	23.9995	56.1411	38.1344	99.5	6.72	8.044	189.8	0.294

Tab. 2 - Results of the multiparametric logs in the point SM1 and SM2 during October 2023

1. By applying the multispectral processing methods used in this study it is possible to carry out highly localized analyses of land use changes over time and quantitatively identify the impact of this variations on sediment supply. The time span analyzed in this study is very broad as the objective was to evaluate the impact of anthropic practices quantitatively and generally on the dynamics of sediment supply and transport at the basin scale;
2. The quantitative estimation of the sedimentary deficit and the identification of the areas where this is most marked allows to objectively plan specific interventions;
3. The possibility of carrying out these procedures on a large scale allows, after having calibrated the model, to expand the calculation to larger areas and evaluate at the scale of a physiographic unit the variation in sedimentary supply and the consequent relationship with the variations in erosion rates in coastal areas.

In the investigated coastal sector, the littoral transport, moving from north to south, is characterised by an average value of about 80,000 m^3/yr. Part of this amount is trapped at the harbour mouth (about 10,000 m^3/yr) and in the longitudinal bar southward from the pier (about 50,000 m^3). These trapped sediments, combined with the low potential sediment supply by the Aron River catchment, represent the main cause of the erosive trend observed in the down-drift sector. For this reason, the handling of sediment trapped in the harbour mouth is essential to try to rebalance the sedimentary equilibrium in the physiographic unit.

The monitoring of the physical-chemical parameters of the seawater column realized in 2 points, consisted of 2 surveys realized during May and October 2023, using the multiparametric probe Ocean Seven 316Plus (Idronaut) (Table1, Table2, Figure 7).

During May 2023 (Table 2), in the point SM1was investigated 6.15m of seawater column with the following results: (*i*) almost constant temperature of 21.7 °C; (*ii*) an electrical conductivity of about 56 mS/cm; (*iii*) salinity around 38 PSU; (*iv*) dissolved oxygen concentration of about 6.6 ppm at top and bottom respectively; (*v*) pH of 8; (*vi*) Eh, starting at 407 mV at the surface, progressively increases up to 434 mV at the bottom; (*vii*) turbidity of 66 NTU close the surface with a decrease up to 46 NTU toward the bottom. In the point SM2, 10.55 m of seawater column were monitored, obtaining: (*i*) almost constant temperature of 22.1 °C; (*ii*) an electrical conductivity of about 190 mS/cm; (*iii*) salinity around 38 PSU; (*iv*) dissolved oxygen concentration varying between 7.6 to 6.6 ppm from top to bottom; (*v*) pH of 7.9; (*vi*) Eh, starting at 208 mV at the surface, progressively decreases up to 189 mV at the bottom; (*vii*) turbidity less than 25 NTU.

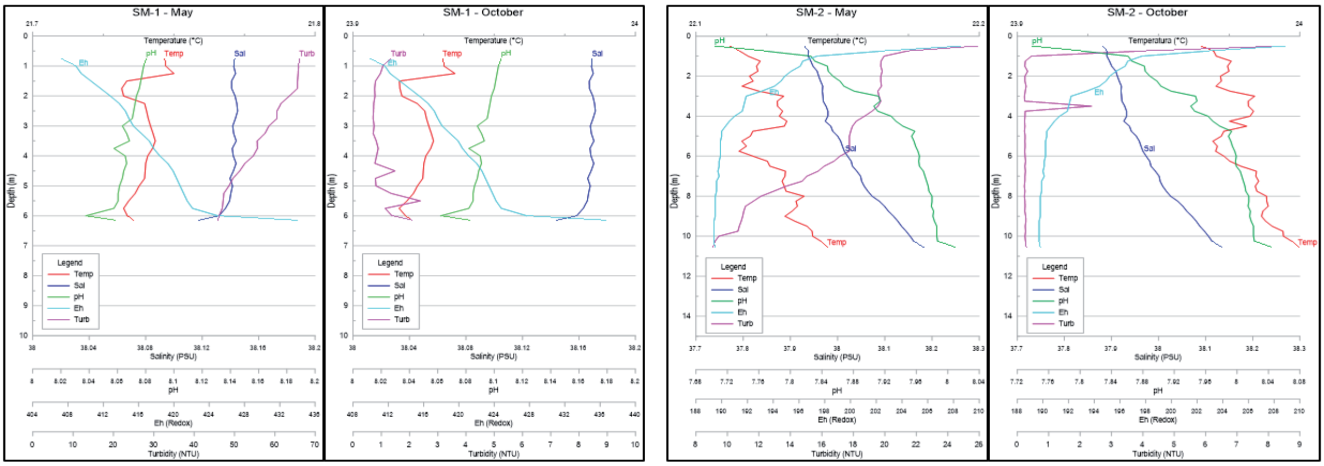

Fig. 7 - May and October multiparametric logs in the point SM1 and SM2

sample	Sediment type	distribution	gravel very coarse	gravel coarse	gravel medium	gravel fine	gravel very fine	sand very coarse	sand coarse	sand medium	sand fine	sand very fine	D_{10} (µm)	D_{50} (µm)	D_{90} (µm)
S1	Sandy Medium Gravel	Bimodal, Poorly Sorted	0%	0%	28,4%	13,9%	18,2%	24%	12,1%	3%	0,4%	0%	771,2	2876,5	9948,5
S2	Sandy Fine Gravel	Bimodal, Poorly Sorted	0%	0%	7%	23%	21,9%	26,6%	14,6%	5,8%	0,8%	0,2%	601,4	2127	7021,1
S3	Very Fine Gravelly Very Coarse Sand	Unimodal, Moderately Sorted	0%	0%	1,5%	3,7%	14,6%	54,5%	18%	3,7%	3%	1%	591,1	1323,4	2798,8
S4	Sandy Very Fine Gravel	Trimodal, Poorly Sorted	0%	0%	17,6%	18,5%	20,1%	25,3%	13,3%	4,4%	0,6%	0,1%	684,1	2448,4	9252,8

Tab. 3 - Results of the grain size analysis

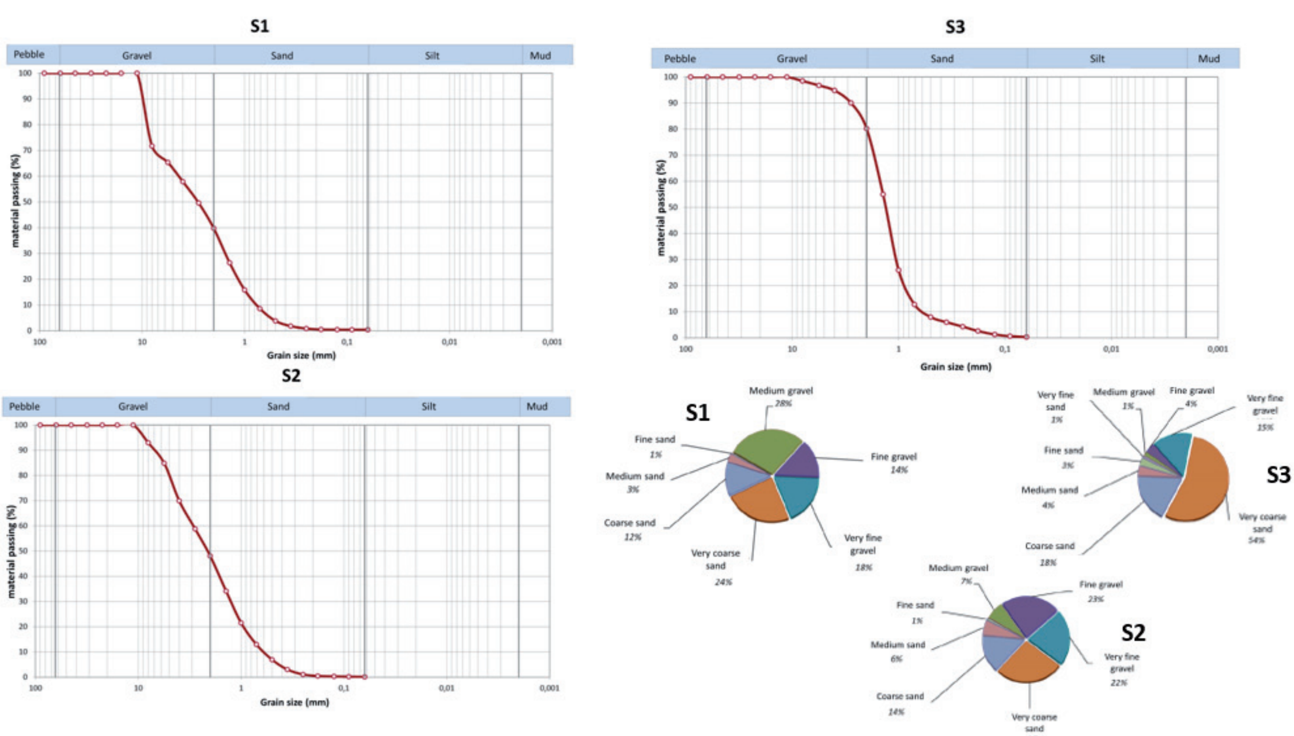

Fig. 8 - Grain size distribution curves

During the survey of October 2023 we obtained the following results for the point SM1 (Table 2): (*i*) temperature of 23.9 °C; (*ii*) electrical conductivity of about 56 mS/cm; (*iii*) salinity around 38.5 PSU; (*iv*) dissolved oxygen concentration of about 6.6 ppm at top and bottom respectively; (*v*) pH of 8.1; (*vi*) Eh varying from 409 mV to 436 mV from top to bottom; (*vii*) turbidity less than 1 NTU. For the point SM2 the results are: (*i*) temperature of 23.9 °C; (*ii*) electrical conductivity of about 56 mS/cm; (*iii*) salinity around 38.1 PSU; (*iv*) dissolved oxygen concentration of about 6.6 ppm (*v*) pH of 8; (*vi*) Eh varying from 189.8 mV to 190.1 mV from top to bottom; (*vii*) turbidity less than 1 NTU.

The seawater column monitoring is strongly influenced by wave climate and environmental conditions of the monitoring points. An example is represented by the fluvial plume. Indeed, the suspended sediment discharged in front of the fluvial mouth can influence many seawater column parameters, particularly turbidity. The effects of fluvial plumes on the seawater turbidity are widely analysed in the recent literature, especially thanks to the approaches based on remote sensing. For example, Tavora *et alii* (2023) developed an algorithm, calibrated with in situ measurements, to calculate the turbidity from satellite images; the authors tested the algorithm in the Patos Lagoon (Brazil), obtaining seawater turbidity values, related to fluvial plumes, up to 50 NTU; Covelli *et alii* (2007) investigated the effects of fluvial plumes on the physico-chemical parameters of seawater in the northern Adriatic Sea (Italy), recording turbidity values, after a river flood, of 50-60 NTU.

In the study area, the turbidity value of up to 60 NTU recorded during May 2023 can be related to the fluvial plume produced by Aron River flood.

The coastal sediment samples were collected at four different points (Fig. 4). In particular, S1 and S2 were sampled in correspondence with the emerged sediment accumulation close to the harbour mouth, while S3 in the submerged area. S4 was sampled in the Lampetia area, northward and up-drift than the Cetraro harbour. The grain-size analysis showed the following features: (*i*) S1 is a poorly sorted sandy medium gravel; (*ii*) S2 is poorly sorted sandy dine gravel; (*iii*) S3 is moderately sorted very fine gravelly/very coarse sand; (*iv*) S4 is poorly sorted sandy very fine gravel.

The results of the grain-size analysis confirm the prevalence in the study area of coarse-grained sediments reported in literature (Cnr, 1997). Furthermore, the new data show that the sediments of emerged area are coarse grained and poorly sorted (bimodal S1 and S2, even trimodal S4), index of poor sediments reworking by waves. Instead, the sediments of submerged area (S3) are reworked by waves as showed by moderated sorting.

On the same 4 sediment samples, ecotoxicological analysis were realized. In detail, the toxicity of the solid fraction of samples (excluding the particles >5 mm of biological, geological, and anthropic origin) was tested by the use of V.fischieri marine bacteria, according to Apat-Icram (2007).

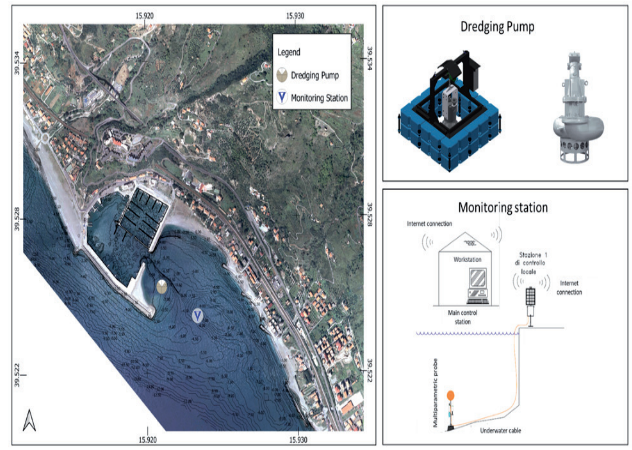

Fig. 9 - Scheme of the bypass and monitoring system

The toxicity of all 4 samples resulted absent/negligible.

Collected data combined with the multidisciplinary approach allowed to design an innovative and sustainable technological solution permitting to contrast the mouth silting and coastline erosion in the down-drift sector.

The beach nourishment in the down drift area with respect to the harbour structure can be realised by means of by-pass systems, which is a low-impact operations recovering the sediment loss due to the coastal dynamic imbalance. The nourishment via a by-pass system normally lasts few days, whereas traditional nourishments using tracks to move the sediment can last longer, implying multiple environmental stresses. A by-pass system implemented with a fixed dredge pump involves the use of a specific electric pump for dredging, properly dimensioned on the distance to be reached. The pump's sizing must ensure the correct velocity of the mixture inside the pipeline, in order to avoid sand settling along the pipeline. An electrical panel controls the pump, which can be manually or timed controlled, by setting the frequency and duration of the pump's operation. A sand pipeline, adequately sized to transport the mixture to the identified accumulation zone is connected to the pump. Being a fixed installation, the pipeline can be buried to avoid interference with maritime traffic.

CONCLUDING REMARKS

The sedimentary balance of the watershed-coast-continuum scale is very important in managing the fluvial and coastal areas. In the Tech4You project (T4Y S2G2PP2), we focused on the silting process affecting the Cetraro harbour mouth, a common problem of a lot of harbours realised in high wave energy areas. In fact, the realization of marine infrastructures usually modifies the wave approach to the coast as well as the longshore current and the sediment drift regime. Usually, the dredging process, involving the removal of sediment in its natural deposited condition by using either mechanical or hydraulic equipment, is carried out. However, dredging implies relevant drawbacks, such as strong impacts on marine flora and fauna mobilization and diffusion of contaminants and pollutants. The aim was to define an innovative and sustainable technological solution to reduce costs and environmental impacts. We characterised the physiographic unit in terms of wave climate and currents and tried to refine the estimation of sedimentary balance. Also the morphology of emerged and submerged areas characterising the sediment's grain size was analysed, and the main physical-chemical parameters (turbidity, temperature, electrical conductivity, salinity, dissolved oxygen, pH, Eh) of the seawater column typically influenced by dredging operations, were monitored. Finally, a bypass system was designed, consisting of a submerged pump installed at the end of the pier on the up-drift side of the harbour. The bypass system allows the movements of the sediments from the trap, created by the harbour structure, to the down-drift coastline. Hence, this system aims to replace the original longshore current in the section of the coast where the littoral current has been interrupted since the harbour building. Simultaneously, the bypass system allows the minimization of the environmental drawbacks produced by the classical dredging operations.

ACKNOWLEDGMENTS

This work was funded by the Next Generation EU - Italian NRRP, Mission 4, Component 2, Investment 1.5, call for the creation and strengthening of 'Innovation Ecosystems', building 'Territorial R&D Leaders' (Directorial Decree n. 2021/3277) - project Tech4You - Technologies for climate change adaptation and quality of life improvement, n. ECS0000009.

REFERENCES

Alvarez-Cuesta M., Toimil A. & Losada I. J. (2021) - *Modelling long-term shoreline evolution in highly anthropized coastal areas. Part 1: Model description and validation.* Coastal Engineering, **169**: 103960. https://doi.org/10.1016/j.coastaleng.2021.103960

Amodio-Morelli L., Bonardi G., Colonna V., Dietrich D., Giunta G., Ippolito F., Liguori V., Lorenzoni S., Paglionico A., Perrone V., Piccarreta G., Russo M., Scandone P., Zanettin Lorenzoni E. & Zuppetta A. (1976) - *L'arco calabro-peloritano nell'orogene Appenninico-Maghrebide.* Memories Italian Geological Society, **17**: 1-60.

Anfuso G. & Del Pozo J.A.M. (2005) - *Towards management of coastal erosion problems and human structure impacts using GIS tools: case study in Ragusa Province, southern Sicily, Italy.* Environ. Geol., **48**: 646-659.

Apat-Icram (2007) – *Manuale per la sedimentazione dei sedimenti marini.* Ministero dell'ambiente e della Tutela del Territotio e del Mare: 72 pp.

Bencivenga M., Nardone G., Ruggiero F. & Calore D. (2012) - *The Italian Data Buoy Network (RON). WIT Trans*. Eng. Sci., **74**: 305.

Bombino G., Barbaro G., D'agostino D., Denisi P., Foti G., Labate A. & Zimbone S. M. (2022) - *Shoreline change and coastal erosion: The role of check dams. First indications from a case study in Calabria, southern Italy.* Catena, **217**: 106494. https://doi.org/10.1016/j.catena.2022.106494

Breiman L. (2001) - *Random Forests.* Machine Learning, **45**: 5-32. https://doi.org/10.1023/A:1010933404324

Brozzetti F., Cirillo D., Liberi F., Piluso E., Faraca E., De Nardis R. & Lavecchia G. (2017) - *Structural style of Quaternary extension in the Crati Valley (Calabrian Arc): Evidence in support of an east-dipping detachment fault.* It. Journ. of Geosci., **136**: 434-453. https://doi.org/10.3301/IJG.2017.11, 2017

Cantasano N., Boccalaro F. & Ietto F. (2023) - *Assessing of detached breakwaters and beach nourishment environmental impacts in Italy: a review.* Environ. Monit. Assess., **195**: 127.

Cantasano N., Pellicone G. & Ietto F. (2017) - *Integrated coastal zone management in Italy: a gap between science and policy*. J. Coast Conserv., **21**: 317-325.

Cianflone G., Conforti M., Soleri S. & Ietto F. (2021) - *Preliminary data on slow-moving landslides-affected urban areas through geological, geomorphological and Insar analysis.* Italian Journal of Engineering Geology and Environment, **1**: 21-33. https://doi.org/10.4408/IJEGE.2021-01.S-02

Cirillo D., Totaro C., Lavecchia G., Orecchio B., De Nardis R., Presti D., Ferrarini F., Bello S. & Brozzetti F. (2022) - *Structural complexities and tectonic barriers controlling recent seismic activity in the Pollino area (Calabria–Lucania, southern Italy) – constraints from stress inversion and 3D fault model building.* Solid Earth, **13**: 205-228.

Cirillo D., Zappa M., Tangari A.C., Brozzetti F. & Ietto F. (2024) - *Rockfall Analysis from UAV-Based Photogrammetry and 3D Models of a Cliff Area.* Drones, **8**: 31. https://doi.org/10.3390/drones8010031

Cnr (1997) - *Atlante delle spiagge italiane*. SELCA, Firenze, Italy.

Congedo L. (2021) - *Semi-Automatic Classification Plugin: A Python tool for the download and processing of remote sensing images in QGIS*. Journal of Open-Source Software, **6**(64): 3172.

Covelli S., Piani R., Acquavita A., Predonzani S. & Faganeli J. (2007) - *Transport and dispersion of particulate Hg associated with a river plume in coastal Northern Adriatic environments.* Marine Pollution Bulletin, **55**(10-12): 436-450.

D'alessandro, L., Davoli L., Lupia Palmieri E. & Raffi R. (1998) - *L'erosione recente delle spiagge calabresi: cause naturali e antropiche.* In: Società Geologica Italiana (Ed) 79° Congresso Società Geologica Italiana, Rome: 373-374 .

D'alessandro, L., Davoli L., Lupia Palmieri E. & Raffi R. (2002) - *Applied geomorphology: theory and practice. In: Allison RJ (ed) Natural and anthropogenic factors affecting the recent evolution of beaches in Calabria (Italy),* Chichister: 397-427.

Dominici R., Larosa R., Viscomi V., Mao L., De Rosa R. & Cianflone G. (2020) – *Yield erosion sediment (YES): a PyQGIS plug-in for the Sediments* *production calculation based on the erosion potential method.* Geosciences, **10**(8): 324.

Filice F., Liberi F., Cirillo D., Pandolfi L., Marroni M. & Piluso E. (2015) - *Geological map of the central area of Catena Costiera: insights into the tectono-metamorphic evolution of alpine belt in Northern Calabria.* Journal of Maps, **11**(1): 114-125. http://www.tandfonline. com/doi/suppl/10.1080/17445647.2014.944877

Foti G., Barbaro G., Barillà G.C., Mancuso P. & Puntorieri P. (2022) - *Shoreline erosion due to anthropogenic pressure in Calabria (Italy).* European Journal of Remote Sensing, **56**(1). Doi: 10.1080/22797254.2022.2140076

Gavrilovic Z. (1988) - *The use of an empirical method (erosion potential method) for calculating sediment production and transportation in unstudied or torrential streams.* In: International Conference on River Regime, Institute for the Development of Water Resources, 'Jaroslav Cerni'.

Gislason P. O., Benediktsson J. A. & Sveinsson J. R. (2006) - *Random forests for land cover classification. Pattern Recognition Letters*, **27**(4): 294-300.

Guiducci F. & Paolella G. (2004) - *Learning from 20 years of design and realization on coastal protection over the Tyrrhenian Calabrian coast.* In: 29th ICCE International Conference on Coastal Engineering. World Scientific Press (Ed), Lisbon: 3826-3838.

Ho T.K. (1995) - *Random Decision Forest*. In: Proceedings of the 3rd International Conference on Document Analysis and Recognition, Montreal, 14-16 August 1995: 278-282.

Hoek E. & Brown E.T. (1997) - *Practical Estimates of Rock Mass Strength*. International Journal Rock Mechanics Mining Science, **34**: 1165-1186.

Iannace A., Vitale S., D'errico M., Mazzoli S., Di Staso,A., Macaione E., Messina A., Reddy S.M., Somma R., Zamparelli V., Zattin M. & Bonardi G. (2007) – *The carbonate tectonic units of northern Calabria (Italy): A record of Apulian paleomargin evolution and Miocene convergence, continental crust subduction, and exhumation of HP LT rocks.* Journal of the Geological Society, **164**: 1165-1186.

Ietto F. (2001) - *Evoluzione delle spiagge tirreniche nord calabresi negli ultimi 50 anni.* Italian Journal of Quaternary Science, **14**(2): 105-116.

Ietto F., Cantasano N. & Pellicone L. (2018) - *A New Coastal Erosion Risk Assessment Indicator: Application to the Calabria Tyrrhenian Littoral (Southern Italy).* Environ. Process., **5**: 201-223.

Ietto F., Salvo F. & Cantasano N. (2014) - *The quality of life conditioning with reference to the local environmental management: a pattern in Bivona country (Calabria, Southern Italy)*. Ocean and Coastal Management: **102**: 340–349.

Ietto F., Conforti M., Tolomei C. & Cianflone G. (2022) - *Village relocation as solution of the landslide risk, is it always the right choice? The case study of Cavallerizzo ghost village (Calabria, southern Italy)*. International Journal of Disaster Risk Reduction, **81**: 103267. https://doi.org/10.1016/j.ijdrr.2022.103267

Lavecchia G., Bello S., Andrenacci C., Cirillo D., Pietrolungo F., Talone D., Ferrarini F., De Nardis R., Galli P., Faure W.J., Sgambato C., Menichetti M., Monaco C., Gambino S., De Guidi G., Barreca G., Carnemolla F. Brighenti F., Giufrida S., Pirrotta C., Carboni F., Ferranti L., Valoroso L., Toscani G., Barchi M.R., Roberts G. & Brozzetti F. (2024) - QUIN 2.0 - *New release of the QUaternary fault strain INdicators database from the Southern Apennines of Italy*. Scientific Data, **11**: 189. https://doi.org/10.1038/s41597-024-03008-6

Liberi F., Piluso E. & Langone A. (2011) - *Permo-Triassic thermal events in the lower Variscan continentalcrust section of the Northern Calabrian Arc, Southern Italy: Insights from petrological data and in situU–Pb zircon geochronology on gabbros*. Lithos,**124**: 291-307.

Lisi I., Bruschi A., Del Gizzo M., Archina M., Barbano A. & Corsini S. (2010) - *Le unità fisiografiche e le profondità di chiusura della costa italiana*. L'Acqua, **2**, Ass. Idrotecnica Italiana (ed.): 35-52.

Mattei M., Cipollari P., Cosentino D., Argentieri A., Rossetti F., Speranza F. & Di Bella L. (2002) - *The Miocene tectono-sedimentary evolution of the southern Tyrrhenian Sea: stratigraphy, structural and palaeomagnetic data from the on-shore Amantea basin (Calabrian Arc, Italy): Tectono-sedimentary evolution of the Amantea basin.* Basin Research, **14**: 147-168.

Piluso E. & Morten L. (2004) - *Hercynian high temperature granulites and migmatites from the CatenaCostiera, northern Calabria, southern Italy.* Periodico di Mineralogia,**73**: 159-172.

Piluso E., Cirrincione R. & Morten L. (2000) - *Ophiolites of the Calabrian Peloritani Arc and their relationships with the crystalline basement (Catena Costiera and Sila Piccola, Calabria, Southern Italy)*. GLOM2000 excursion guide-book. Ofioliti, **25**: 117-140.

Romano B., Zullo F., Fiorini L., Marucci A. & Ciabò S. (2017) - *Land transformation of Italy due to half a century of urbanization*. Land Use Policy, **67**: 387-400. https://doi.org/10.1016/j.landusepol.2017.06.006

Stancheva M., Rangel-Buitrago N., Anfuso G., Palazov A., Stanchev H. & Correa I. (2011) - *Expanding level of coastal armouring: case studies from different countries*. J. Coast. Res., SI **64**: 1815-1819.

Stronkhorst J., Levering A., Hendriksen G., Rangelbuitrago N. & Appelquist L. R. (2018) - *Regional coastal erosion assessment based on global open access data: A case study for Colombia. Journal of Coastal Conservation*, **22**(4): 1-12. https://doi.org/10.1007/s11852-018-0609-x

Tangari A. C., Le Pera E., Andò S., Garzanti E., Piluso E., Marinangeli L. & Scarciglia F. (2021) - *Soil-formation in the central Mediterranean: Insight from heavy minerals.* Catena, **197**. Doi: 10.1016/j.catena.2020.104998, 2021.

Tavora J., Goncalves G.A., Fernandes E.H., Salama M.S. & Van Der Wal D. (2023) - *Detecting turbid plumes from satellite remote sensing: State-of-art thresholds and the novel PLUMES algorithm*. Front. Mar. Sci., **10**: 1215327. Doi:10.3389/fmars.2023.1215327

Zemljic M. (1971) - *Calcul du debit solide – evaluation de la vegetation comme un des facteurs antierosifs*. In: International Symposium Interpraevent, Villach, Austria.

Received January 2024 - Accepted March 2024